

Validation of a biomechanical heart model using animal data with acute myocardial infarction

Radomir Chabiniok, Dominique Chapelle, Pierre-François Lesault, Alain Rahmouni, Jean-François Deux

▶ **To cite this version:**

Radomir Chabiniok, Dominique Chapelle, Pierre-François Lesault, Alain Rahmouni, Jean-François Deux. Validation of a biomechanical heart model using animal data with acute myocardial infarction. CI2BM09 - MICCAI Workshop on Cardiovascular Interventional Imaging and Biophysical Modelling, Sep 2009, London, United Kingdom. 9 p. inria-00418373

HAL Id: inria-00418373
https://inria.hal.science/inria-00418373

Submitted on 18 Sep 2009

HAL is a multi-disciplinary open access archive for the deposit and dissemination of scientific research documents, whether they are published or not. The documents may come from teaching and research institutions in France or abroad, or from public or private research centers.

L'archive ouverte pluridisciplinaire **HAL**, est destinée au dépôt et à la diffusion de documents scientifiques de niveau recherche, publiés ou non, émanant des établissements d'enseignement et de recherche français ou étrangers, des laboratoires publics ou privés.

Validation of a biomechanical heart model using animal data with acute myocardial infarction

R. Chabiniok†, D. Chapelle†, P.F. Lesault‡, A. Rahmouni‡, J.F. Deux‡

†INRIA Rocquencourt, France
‡Henri Mondor Hospital, Créteil, France

Abstract. In this paper, we validate a biomechanical heart model with animal data providing a controlled infarct condition with a follow-up over several weeks. First, we set up the personalized model using data coming from the healthy animal, and we show that the simulations compare accurately with the measured data, both for the tissue motion and for the blood pressures. Then, we demonstrate that we can also adequately represent the behavior of the acutely infarcted heart by changing only the parameters directly related to the pathology, and to the physiological state of the subject during the exams.

Key words: Heart modeling; Biomechanics; MRI

1 Introduction

Personalized – or patient-specific – biomechanical modeling of the heart represents a tremendous challenge for clinical applications [9]. In such endeavors, the predictive capabilities of the model – namely, its ability to adequately simulate the various phenomena of concern in a given clinical application once the relevant parameters have been calibrated – is crucial, not only to represent normal behavior, but also pathologies, since personalized modeling aims at diagnosis and prognosis assistance.

The present work pertains to the clinical assessment of a biomechanical heart model used to represent the effect of acute myocardial infarction, with animal data providing a controlled infarct condition with a follow-up over several weeks. First, we set up the personalized model using data coming from the healthy animal. We will show that the model simulations compare quite accurately with the measured data, both for the tissue motion and for the blood pressures. The second part deals with the modeling of an acute myocardial infarction using the same biomechanical model with locally modified material properties, with a detailed assessment of the simulated indicators.

2 Experimental data

The experimental data consisted of animal data obtained with a farm pig of 25kg. The in-vivo study was approved by the Institutional Animal Care and

Use Committee of "Faculté de Créteil", France. Animals were housed and cared according to European Union Standards. Before each data acquisition, the animal was premedicated with intramuscular Ketamin (15 mg/kg), anesthetized with Propofol (0.35 mg/kg intravenous bolus and 0.05 mg/kg/min continuous infusion), intubated and ventilated, see [4] for the detailed experimental protocol. The subject was examined and data acquired once in a baseline condition (physiological heart beat).

Then, antero-septal myocardial infarction was induced by a 120-min occlusion of the mid-left anterior descending coronary artery, using a balloon catheter, followed by reflow. Such an occlusion led to an extended myocardial infarction, as was proven in the follow-up by the late-enhancement MR images. The animal was re-examined 10 and 38 days after the infarct creation. The corresponding stages are referred to as baseline, T0+10 and T0+38 in the sequel. The T0+10 data acquisition corresponds to the acute stage (edematous necrotic tissue with only slightly diminished wall thickness), while at T0+38 we could already expect – and indeed observed – thinning of the LV wall (caused by resorption of the necrosis and tissue remodeling).

The data-sets consist of non-invasive cardiac MRI and invasive measurement or pressures in the cardiac cavities:

- Cardiac MRI (Philips Achieva 3T with 32-channel phased-array cardiac coil)
  - Cine sequences in retrospective ECG gating: short axis views covering the whole volume of the heart and several long axis views.
  - Tagged cine data in prospective ECG gating.
  - Late enhancement images (after creation of the infarct only) acquired 10 minutes after injection of a MR contrast agent (gadolinium chelate).
- Invasive measurement of pressures in the cardiac cavities and large arteries, performed 30-60 minutes before image acquisition: namely, left ventricle, aorta, right atrium, right ventricle, pulmonary artery and pulmonary capillary wedged pressure. Each pressure was taken in breath-hold (controlled by the ventilator).

3 Biomechanical model

3.1 Model formulation

The biomechanical model used here – detailed in [8] – is based on physiological considerations and is consistent with essential thermomechanical requirements (energy balances in particular), preserved from the continuous dynamical equations to the discrete versions used for numerical simulations. We also refer to [2] for another example of some physiological simulations performed within the same modeling framework.

The heart tissue is modeled as an active 3D viscoelastic material. It contains a 1D active component in the direction of the myocardial fibers, modeled according to [1]. The external blood circulations are represented by Windkessel models [6].

3.2 Anatomical model

The cardiac anatomy was obtained by segmenting a diastolic time frame MR image preceding the atrial contraction, a state considered as a reference (stress-free) configuration of the heart. Segmentation of the left and right heart ventricles in this particular time-frame image was performed manually using the CardioViz3D software [11]. Then a computational mesh was built in the segmented geometry using the Yams and GHS3D meshing tools [3], see the resulting mesh in Fig. 1.

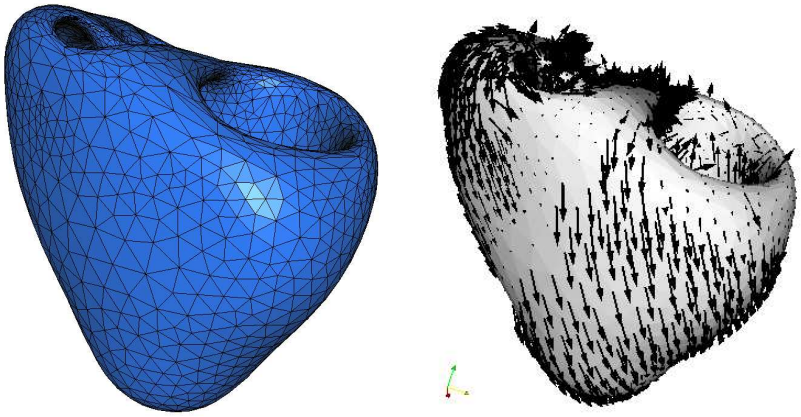


Fig. 1. Computational mesh for baseline (left) and generic fibers prescribed in the mesh (right).

Fiber directions – needed in the biomechanical model as privileged directions of contraction – were prescribed in the same anatomical model based on general anatomical knowledge [10]: -60/60 degrees in LV, -50/50 degrees in RV, from epicardium to endocardium, see Fig. 1.

3.3 Calibration of mechanical parameters of the model

The model parameters were calibrated for the baseline condition, namely, in the healthy heart. Tissue contractility and passive tissue stiffness were calibrated to obtain good adequacy of the ventricular pressures and global motion compared to the measured data, including the LV pressure time derivative dp/dt and the ejection fractions. Correct peak ventricular pressure and the pressures in large arteries (aorta and pulmonary artery) were obtained by calibrating capacitances and resistances of the Windkessel models.

3.4 Modeling of the infarct

For each of the post-infarct stages, a new anatomical model was created by segmenting MR images in the same way as for the baseline condition. Addi-

tionally, we segmented the infarcted tissue using late enhancement images and projected it in the mesh (see Fig. 2). The initial aortic pressure and values of atrial pressures were taken from the measurements. The heart rate and duration of the heart contraction were adjusted to the MR image data. In order to represent the impact of the infarct on the tissue, we decreased the contractility and increased the passive stiffness in the regions concerned, as segmented from the late-enhancement MR images. All other parameters of the model were kept exactly as in the baseline simulation. We summarize the parameter variations in Table 1.

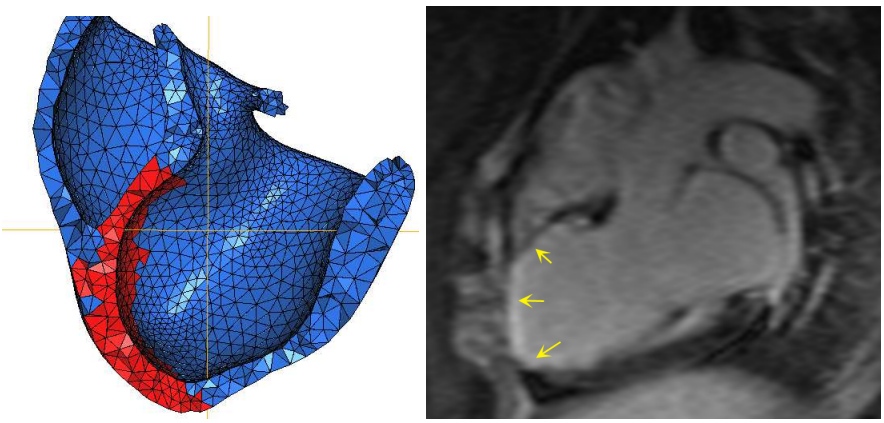


Fig. 2. Infarct at T0+38: in the mesh (left, in red) as segmented from the late enhancement MR images (right, yellow arrows).

Parameter	Baseline	T0+10	T0+38
contractility	σ_0	$\sigma_0/5$ (infarcted region)	$\sigma_0/5$ (infarcted region)
stiffness	κ_1	$\kappa_1 * 10$ (infarcted region)	$\kappa_1 * 10$ (infarcted region)
minimum aortic pressure	73 mmHg	53 mmHg	89 mmHg
activation duration	220 ms	275 ms	246 ms
left atrial pressure	12 mmHg	12 mmHg	20 mmHg

Table 1. Parameter values modified in infarction model

3.5 Results

In Figure 3 we compare the simulated and measured pressures and volumes in the main compartments, for each of the three stages.

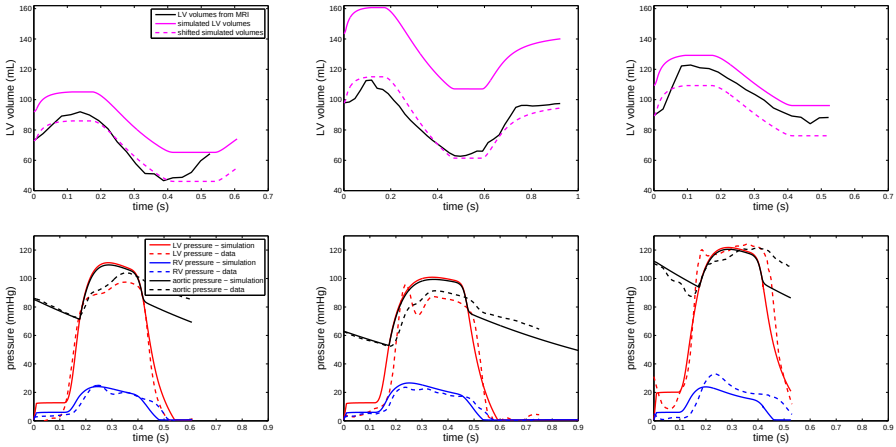


Fig. 3. Volumes and pressures: baseline (left), T0+10 (in the middle), T0+38 (right).

The heart motion is more accurately confronted with experimental data by plotting the model contours within MR images, see Figs. 4, 5 and 6. We also produced synthetic tagged images from the model simulations, which are compared with experimental ones in Fig. 7.

4 Discussion

Left ventricular volumes plotted in Fig. 3 are not directly accurate. This is mainly due to the fact that simulated and measured volumes are not computed based on the same regions. Simulated volumes take into account the model cavities approximately up to the valve plane, whereas measured volumes are taken in a truncated anatomy between two fixed sections in the image space. Hence, in Figure 3 we also show a shifted simulated volume to account for this difference. Nevertheless, these curves are mainly to be considered to assess the timings of the cardiac cycle, as detailed motions are directly assessed by comparing images and model contours.

The simulated and measured pressure values are found to be in very good overall agreement at the three stages. We note that the systolic pressure increase rate (dp/dt) is somewhat underestimated in the simulations at the infarcted stages. This may be due to an increase in the contractility resulting from growth combined with an adaptation mechanism of the cardiovascular system. In a larger study a mini-pig should be used (instead of a young subject) to avoid the influence of growth and young age specificities in the post-infarct follow-up.

The comparison of model contours with image also demonstrates a very good adequacy of the simulated motion. The main discrepancy is to be observed near the base, which is due to artificial boundary conditions which must be imposed in

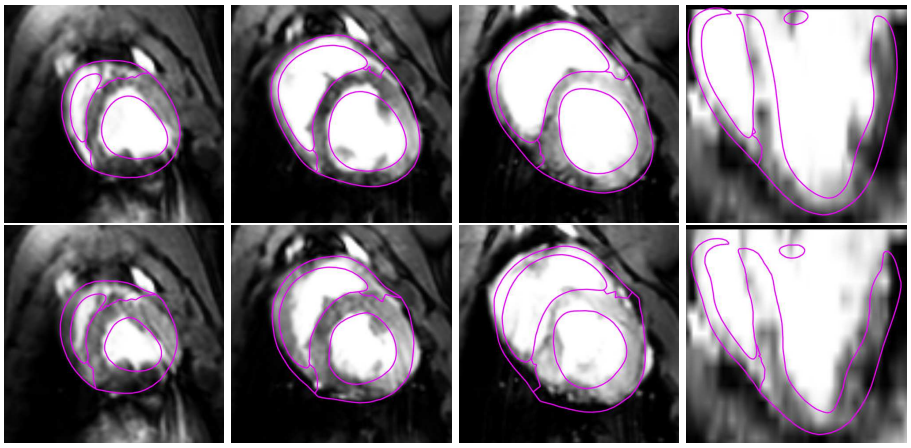


Fig. 4. Baseline: Initial configuration (top) and end-systolic time frame (bottom), with model contours in purple.

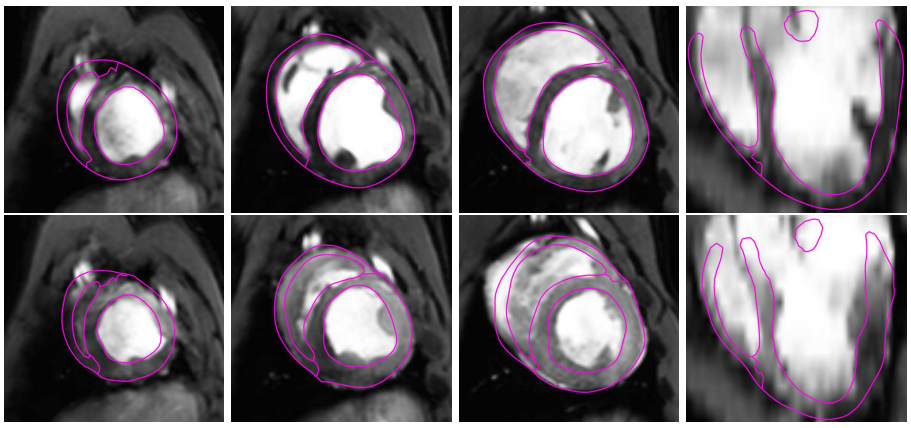


Fig. 5. T0+10: Initial configuration (top) and end-systolic time frame (bottom), with model contours in purple.

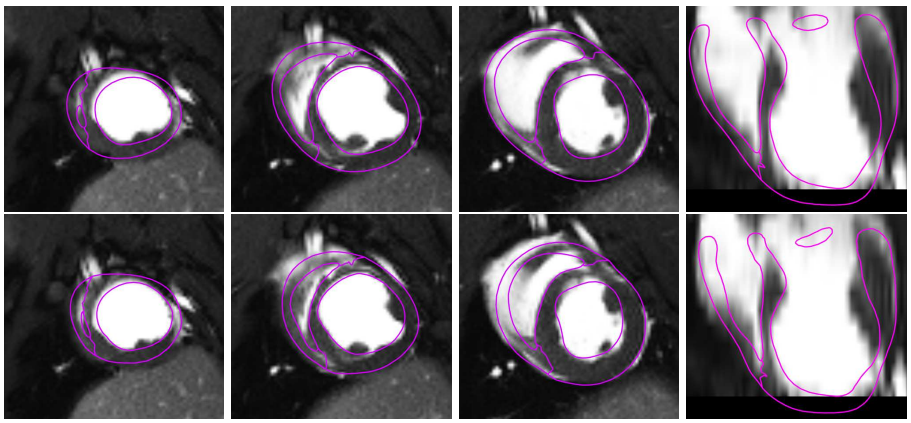


Fig. 6. T0+38: Initial configuration (top) and end-systolic time frame (bottom), with model contours in purple.

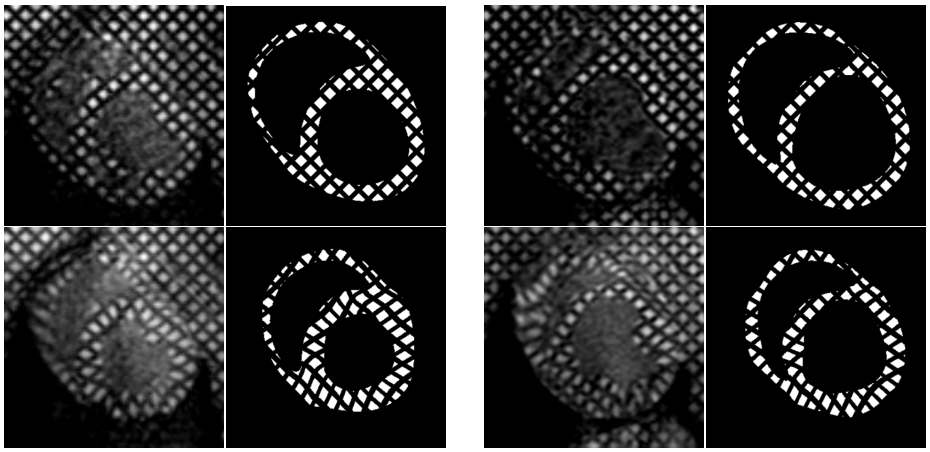


Fig. 7. Comparison of MR and synthetic tagged images for baseline (left four images) and T0+10 stage (right four images). End-diastolic time frames are displayed in the upper row, end-systolic time frames in the lower row.

this region to account for the truncated part of the anatomy. The akinetic region (in the anterior and antero-septal apical and mid-cavity segments) is clearly visible – both in the images and in the model – and is even more pronounced at T0+38.

The synthetic tagged images in the baseline clearly show that the simulation of the healthy heart is very accurate in all segments of the left ventricle. The akinetic region seen in the T0+10 clinical tagged images is also well captured in the synthetic tagged images, although the anterior segment shows some slight thickening in the simulation. This is likely to be due to the difficulty of accurately assessing the extension of the infarcted region in the acute stage with the late enhancement images.

Therefore, according to the various indicators considered, by changing just a few relevant physiological parameters we obtain a very good adequacy between simulations and experimental data.

5 Further perspectives

This infarct model was considered in a case without any other co-morbidity factor. For a real patient, other factors (e.g. electrical activation pathologies) should be taken into account in the model. In addition, other artificial infarct protocols may be used, in particular since reversible occlusion may have a limited impact (tissue stunning, see [5]). From the follow-up of the animal in the present case, we can see that the tissue was really massively infarcted. Furthermore, we prefer reversible occlusion since it is more usual in patients in today's treatments of the myocardial infarction.

We emphasize that other physical variables can be obtained from the model simulations, such as stresses which may be essential to better understand some physiological phenomena involved in tissue remodeling, in particular.

A detailed study of the influence of the key physical parameters – namely, contractility and tissue stiffness – should be undertaken. This may be automatized by performing estimation of these parameters [9]. The experimental data can also be used in a *global estimation* procedure to correct the various model variables, hence to obtain improved motion fields and pressures, see [7]. This is in fact necessary to obtain a correct estimation of the parameters.

6 Conclusions

We showed that our biomechanical model of the heart can be personalized and calibrated to accurately reproduce the pressures and motion measured in a healthy animal subject. Then, we demonstrated that we can also adequately represent the behavior of the acutely infarcted heart by changing only the parameters directly related to the pathology (contractility and stiffness in the infarcted area) and to the physiological state of the subject during the exam (atrial and aortic blood pressure, heart rythm).

Of course, a more extensive validation – with numerous animal and human data-sets – is required to show that this personalized modeling strategy can be valuable in clinical applications. Further perspectives include automated estimation of the relevant physiological parameters, and the modeling of other types of pathologies, including with multiple co-morbidity factors.

Acknowledgments: The research leading to these results has received funding from the European Community's Seventh Framework Program (FP7/2007-2013) under grant agreement number 224495 (euHeart project). The authors also acknowledge support by INRIA through its large scope initiative CardioSense3D. In addition, they wish to thank Jaroslav Tintera (IKEM Prague) for his help with the MRI sequences, and Matthew Sinclair for his assistance with the biomechanical simulations.

References

1. J. Bestel, F. Clément, and M. Sorine. A biomechanical model of muscle contraction. In *Lectures Notes in Computer Science*, volume 2208. Eds W.J. Niessen and M.A. Viergever, Springer-Verlag, 2001.
2. D. Chapelle, M.A. Fernández, J.F. Gerbeau, P. Moireau, and N. Zemzemi. Numerical simulation of the electromechanical activity of the heart. In *FIMH'09: Functional Imaging and Modeling of the Heart*, Nice, 2009.
3. P.J. Frey and P.L. George. *Mesh generation application to finite elements.* Wiley, London, 2008.
4. J. Garot, T. Unterseeh, E. Teiger, S. Champagne, B. Chazaud, R. Gherardi, L. Hittinger, P. Guéret, and A. Rahmouni. Magnetic resonance imaging of targeted catheter-based implantation of myogenic precursor cells into infarcted left ventricular myocardium. *Journal of the American College of Cardiology*, 41(10), 2003.
5. R.A. Kloner and R.B. Jennings. Consequences of brief ischemia: Stunning, preconditioning, and their clinical implications, part 1. *Circulation*, 104:2981–2989, 2001.
6. D.A. MacDonald. *Blood Flow in Arteries.* Edward Harold Press, 1974.
7. P. Moireau, D. Chapelle, and P. Le Tallec. Joint state and parameter estimation for distributed mechanical systems. *Computer Methods in Applied Mechanics and Engineering*, 197:659–677, 2008.
8. J. Sainte-Marie, D. Chapelle, R. Cimrman, and M. Sorine. Modeling and estimation of the cardiac electromechanical activity. *Computers & Structures*, 84:1743–1759, 2006.
9. M. Sermesant, Ph. Moireau, O. Camara, J. Sainte-Marie, R. Andriantsimiavona, R. Cimrman, D.L. Hill, D. Chapelle, and R. Razavi. Cardiac function estimation from mri using a heart model and data assimilation: advances and difficulties. *Med. Image Anal.*, 10(4):642–656, 2006.
10. S. Standring. *Gray's Anatomy.* Churchill Livingstone, 2008.
11. N. Toussaint, T. Mansi, H. Delingette, N. Ayache, and M.: Sermesant. An integrated platform for dynamic cardiac simulation and image processing: Application to personalised tetralogy of Fallot simulation. In *Proc. Eurographics Workshop on Visual Computing for Biomedicine (VCBM).* Delft, The Netherlands, 2008.